2016 International Symposium on Nonlinear Theory and Its Applications,
NOLTA2016, Yugawara, Japan, November 27th-30th, 2016

Wave-chaos-induced single-frequency lasing in microcavities

Satoshi Sunada[1], Susumu Shinohara[2], Takehiro Fukushima[3], and Takahisa Harayama[4]

[1]Faculty of Mechanical Engineering, Institute of Science and Engineering, Kanazawa University
Kakuma-machi Kanazawa, Ishikawa 920-1192, Japan
[2]NTT Communication Science Laboratories, NTT Corporation
2-4 Hikaridai Seika-cho Soraku-gun, Kyoto 619-0237, Japan
[3]Department of Information and Communication Engineering, Okayama Prefectural University
111 Kuboki Soja, Okayama 719-1197, Japan
[4]Department of Applied Physics, School of Advanced Science and Engineering, Waseda University
3-4-1 Okubo, Shinjuku-ku, Tokyo 169-8555, Japan
Email: sunada@se.kanazawa-u.ac.jp

Abstract—We experimentally and numerically demonstrate that stable single-frequency (i.e., single-mode) lasing can be achieved in microcavities that have wave-chaotic modes. The single-frequency lasing is explained as a result of strong competitive interactions among wave-chaotic modes.

1. Introduction

Various active devices ranging from musical instruments to lasers generate oscillating states with well-defined frequencies from the interplay between resonator geometry and an active nonlinear element [1, 2]. Understanding and controlling the formation of such self-organized oscillating states is important in device physics and related applications. As a specific example, two-dimensional (2D) microcavity lasers have attracted considerable attention over the past decades [3, 4, 5]. Depending on the cavity shapes, they can exhibit a variety of lasing states through the interaction between the light field and active gain material [2]. The studies of 2D microcavity lasers have led to a wide range of applications, including low-threshold microlasers with unidirectional emission [6], low-coherence microlasers [7], and fast random signal generation [8]. Moreover, 2D microcavity lasers have served as a platform for experimentally addressing fundamental issues such as quantum/wave chaos in open systems [5] and non-Hermitian physics [9, 10].

The lasing emission patterns and spectra are fundamental and important characteristics of 2D microcavity lasers. Previous experimental and theoretical studies have shown that the lasing emission patterns can be well characterized by resonant modes, which are determined only by the cavity shape and refractive index [3, 4]. Meanwhile, the spectral characteristics are still poorly understood because nonlinear interaction among resonant modes plays an crucial role in determining lasing frequencies.

In this presentation, we report our recent finding on a relationship between shapes of 2D microcavities and the lasing frequencies [11]. We show that stable single-frequency (i.e., single-mode) lasing can be achieved in fully chaotic cavities, where all of the internal ray orbits are chaotic in a ray optics picture and the spatial patterns of the modes are wave-chaotic, whereas multi-frequency (i.e., multimode) lasing is exhibited in non-chaotic cavities. The achievement of single-mode lasing in fully chaotic cavities is explained as a result of strong mode competition among wave chaotic modes.

2. Fully chaotic and non-chaotic microcavities

A specific shape of the fully chaotic cavity that we study here is a stadium [12], which is widely used for classical and quantum chaos studies. As shown in Fig. 1(a), the stadium cavity consists of two straight lines of length l and two half circles of radius R. We define the aspect ratio parameter $p = W/L$, where $W = 2R$ is the length of the minor axis and $L = 2R + l$ is the length of the major axis. For the non-chaotic cavity, we focus on the elliptic cavity defined in Fig. 1(b). It is known that a closed elliptic cavity is an integrable system [13], thus exhibiting no chaotic behavior. In the same manner as for the stadium cavity, we define the aspect ratio parameter for the elliptic cavity as $p = B/A$, where A and B are the lengths of the major and minor axes, respectively.

We fabricated semiconductor microcavities with the stadium and elliptic cavities by applying a reactive-ion-etching technique to a graded index separate-confinement-heterostructure (GRIN-SCH) single-quantum-well $GaAs/Al_xGa_{1-x}As$ structure grown by MOCVD (See Ref. [14] for details on the layer structures and fabrication process). The fabricated lasers are shown in Figs. 1(c) and 1(d). In our experiments, the lasers were soldered onto aluminum nitride submounts at 20 ± 0.1 °C and electrically driven with cw current injection. The optical outputs were collected with anti-reflection-coated lenses and coupled to a multimode optical fiber via a 30-dB optical isolator.

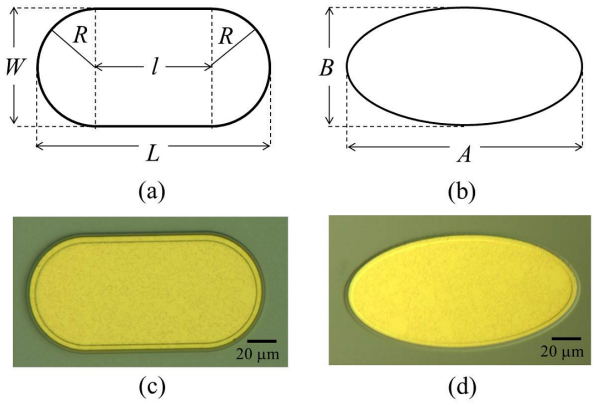

Figure 1: (a) Stadium cavity and (b) elliptic cavity. (c)(d) Optical microscope images of the fabricated lasers, where both cavities have an area $S = 8748\,\mu\text{m}^2$ and an aspect ratio $p = 0.5$.

3. Experimental results

Figure 2 shows typical lasing wavelength spectra for the stadium cavity laser and elliptic cavity lasers. Because the lasing wavelength λ is related to a frequency f by $c = f\lambda$, where c is the light velocity, we dicuss the spectral characteristics in the wavelength regime. As shown in Fig. 2, there is a remarkable difference in the number of peaks between the two lasers. The spectrum of the stadium cavity laser exhibits only a single sharp peak, suggesting single frequency (single-mode) lasing, despite the fact that the number of modes within the gain band is more than a few thousand because of the large cavity area. Meanwhile, the spectrum of the elliptic cavity laser always exhibits multiple peaks, i.e., multimode lasing.

We systematically investigated the spectral characteristics of the two lasers with various cavity areas S and aspect ratios p. Figure 3 shows the number of peaks whose intensities were larger than -20 dB of the maximum peak intensity in each spectrum as a function of the current I normalized by the threshold current I_{th} for each laser. The spectra of the elliptic cavity lasers always exhibit multiple peaks, i.e., multimode lasing, and the number of peaks increases as I increases. On the other hand, the spectra of the stadium cavity lasers always exhibit a single peak, i.e., single-mode lasing, regardless of the cavity areas and aspect ratios, and the single-mode lasing is maintained even for high injection current values I. However, as a slight exception, we observed two peaks for the stadium cavity laser for $I/I_{th} = 2.1$ and 2.7 in Fig. 3. We attribute this to mode hopping caused by a thermal effect of the current injection, such as a gain shift and a change in the refractive index.

4. Discussion and Analysis

The above results indicate that strong suppression of multimode lasing is a common feature of stadium cavity

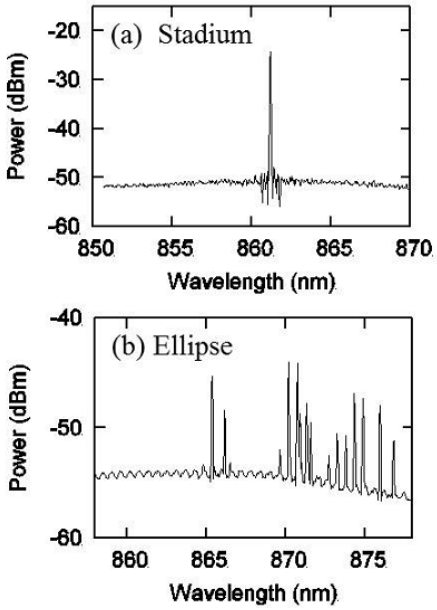

Figure 2: Spectra of the stadium and elliptic cavity lasers with a cavity area $S = 8748\,\mu\text{m}^2$ and an aspect ratio $p = 0.5$ for the injection current $I = 140$ mA. The threshold currents of the stadium and elliptic cavity lasers were 74 and 34 mA, respectively.

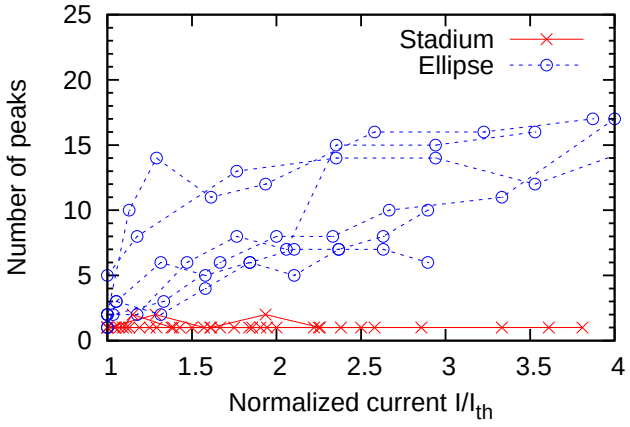

Figure 3: Injection current dependence of the number of peaks in the spectra of the stadium cavity lasers (red crosses) and the elliptic cavity lasers (blue circles) with cavity area $S = 4463$, 6427, and 8748 μ m^2 and aspect ratios in a range of $0.3 \le p \le 1$.

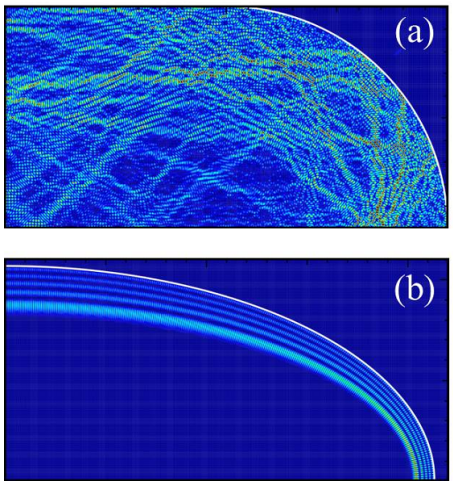

Figure 4: (a) Spatial intensity pattern of a low-loss mode in a quarter of the stadium cavity. (b) Spatial intensity pattern of a low-loss mode in a quarter of the elliptic cavity.

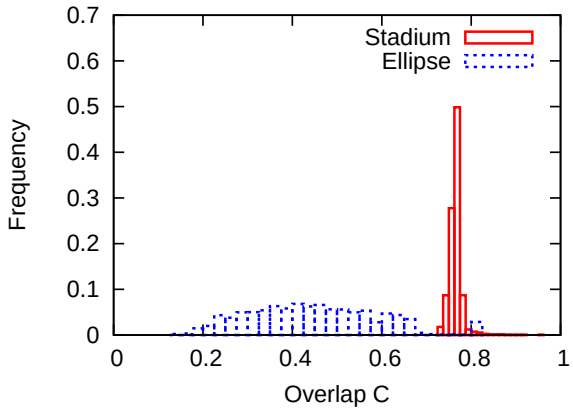

Figure 5: Histogram of overlap C defined by Eq. (1) between two low-loss modes for the stadium cavity (solid) and elliptic cavity (dotted).

lasers. As discussed in Refs. [15, 16], a competitive interaction occurs among modes that are overlapped not only spectrally but also spatially. In a fully chaotic cavity, modes typically have complex spatial patterns that spread throughout the entire cavity due to the ray dynamical property [for a typical example, see Fig. 4(a)], and therefore result in large spatial overlaps with other modes. Actually, previous numerical simulations of stadium cavity lasers demonstrated a strong selection of lasing modes owing to a competitive interaction [17, 18, 19]. On the other hand, non-chaotic cavities typically support spatially localized modes [e.g., Fig. 4 (b)]. Interestingly, different modes are localized in different areas. Thus, when the spatial overlap among modes is small, the competition among them can be avoided. Indeed, the simultaneous lasing of multiple modes for a non-chaotic cavity laser with a circular shape was numerically demonstrated in Ref. [20].

To quantify the spatial overlaps between two modes in a cavity, we introduce the following cross-correlation for the amplitude distributions of resonance modes:

$$C = \frac{\int |\phi(\boldsymbol{r})|\,|\psi(\boldsymbol{r})|\,w(\boldsymbol{r})d\boldsymbol{r}}{\sqrt{\left(\int |\phi(\boldsymbol{r})|^2\,w(\boldsymbol{r})d\boldsymbol{r}\right)\left(\int |\psi(\boldsymbol{r})|^2\,w(\boldsymbol{r})d\boldsymbol{r}\right)}}, \qquad (1)$$

where $\phi(\boldsymbol{r})$ and $\psi(\boldsymbol{r})$ are the modal wave functions and $w(\boldsymbol{r})$ represents a pumping region. For uniform pumping, $w(\boldsymbol{r}) = 1$ inside the cavity, whereas $w(\boldsymbol{r}) = 0$ outside. The correlation is essentially similar to a spatial contribution to the cross-gain saturation (i.e., intensity cross-correlation) between two modes [15, 16, 21]. Using the boundary element method [22], we calculated the resonances of the stadium and elliptic cavities with $p = 0.5$, imposing a refractive index of 3.3 inside the cavities and transverse electric (TE) polarization. Because of computational power limitations, we set a size parameter $2\pi R/\lambda \approx 100$, where R and λ are the characteristic radius and wavelength, respectively. This size parameter value is smaller than that of a real laser cavity used in the experiments but is sufficiently large to discuss the properties of the wave functions in the short-wavelength regimes [23]. We obtained approximately 100 low-loss modes with a quality factor $Q \geq 3000$ for the stadium cavity, whereas $Q \geq 3 \times 10^5$ for the elliptic cavity. Typical examples of the wave functions for stadium and elliptic cavities are shown in Fig. 4.

Figure 5 shows the histogram of the spatial overlap C between two low-loss modes in stadium and elliptic cavities. The C-values for the stadium cavity are distributed around 0.77. In contrast, the C-values for the elliptic cavity are widely distributed with a mean value of 0.45. The relatively low C-values come from the small spatial overlaps between the localized modes. In particular, the overlaps are small between two modes with different radial mode numbers n_r, which characterize the number of field maxima in the radial direction. For instance, the C-value between the modes with $n_r = 5$ and $n_r = 1$ was only 0.14. As seen in Fig. 2 (b), the lasing peaks in the spectra of the elliptic cavity laser are not always equally spaced. This result means that modes with different n_r-values were involved in the lasing, which supports our interpretation of the relation between the spatial overlaps and the spectral characteristics.

5. Conclusion

We experimentally investigated the difference in the spectral characteristics between fully chaotic cavity lasers with a stadium shape and non-chaotic cavity lasers with an elliptic shape. In the stadium cavity lasers, only a single mode was excited at high pumping regimes regardless of the size and aspect ratio, whereas many modes were excited in the elliptic cavity lasers. The strong suppression of multimode lasing observed in the stadium cavity lasers can

be explained by the large spatial overlaps among the low-loss modes. Because a common feature of modes in a fully chaotic cavity is the spatial pattern that spreads throughout the entire cavity, we expect that the modal suppression leading to single-mode lasing is a universal feature of fully chaotic cavity lasers.

Acknowledgments

This work was supported by JSPS KAKENHI Grant Numbers 26790056 and 16K04974.

References

[1] H. Haken, *Synergetics. An Introduction, Nonequilibrium Phase Transitions and Self-organization in Physics, Chemistry, and Biology,* (Springer, Berlin, 1977).

[2] T. Harayama and S. Shinohara, Laser Photonics Rev. **5**, 247 (2011).

[3] J. U. Nöckel and A. D. Stone, Nature **385**, 45 (1997).

[4] C. Gmachl, F. Cappasso, E. E. Narimanov, J. U. Nöckel, A. D. Stone, J. Faist, D. L. Sivco, and A. Y. Cho, Science **280**, 1556 (1998).

[5] H. Cao and J. Wiersig, Rev. Mod. Phys. **87**, 61 (2015).

[6] X.-F. Jiang, C.-L. Zou, L. Wang, Q. Gong, and Y.-F. Xiao, Laser Photonics Rev. **10**, 40 (2016).

[7] B. Redding, A. Cerjan, X. Huang, M. L. Lee, A. D. Stone, M. A. Choma, and H. Cao, Proc. Natl. Acad. Sci. USA **112**, 1304 (2015).

[8] S. Sunada, T. Fukushima, S. Shinohara, T. Harayama, K. Arai, and M. Adachi, Appl. Phys. Lett. **104**, 241105 (2014).

[9] M. Liertzer, L. Ge, A. Cerjan, A. D. Stone, H. E. Türeci, and S. Rotter, Phys. Rev. Lett. **108**, 173901 (2012); M. Brandstetter, M. Liertzer, C. Deutsch, P. Klang, J. Schöberl, H. E. Türeci, G. Strasser, K. Unterrainer, and S. Rotter, Nat. Commun. **5**, 4034 (2014).

[10] B. Peng, S. K. Özdemir, S. Rotter, H. Yilmaz, M. Liertzer, F. Monifi, C. M. Bender, F. Nori, L. Yang, Science **346**, 328 (2014).

[11] S. Sunada, S. Shinohara, T. Fukushima, and T. Harayama, Phys. Rev. Lett. **116**, 203903 (2016).

[12] L. A. Bunimovich, Commun. Math. Phys. **65**, 295 (1979).

[13] M. V. Berry, Eur. J. Phys. **2**, 91 (1981).

[14] T. Fukushima and T. Harayama, IEEE J. Sel. Top. Quantum Electron. **10**, 1039 (2004).

[15] M. Sargent III, M. O. Scully, and W. E. Lamb, Jr, *Laser Physics*, (Addison-Wesley Pub., Massachusetts, 1974).

[16] M. Sargent III, Phys. Rev. A **48**, 717 (1993).

[17] S. Sunada, T. Fukushima, S. Shinohara, T. Harayama, and M. Adachi, Phys. Rev. A **88**, 013802 (2013).

[18] S. Sunada, T. Harayama, and K. S. Ikeda, Phys. Rev. E **71**, 046209 (2005).

[19] T. Harayama, S. Sunada, and K. S. Ikeda, Phys. Rev. A **72**, 013803 (2005).

[20] S. Sunada, T. Harayama, and K. S. Ikeda, Nonlinear Phenom. Complex Syst. **10**, 1 (2007).

[21] M. Yamada, IEEE J. Quantum Electron. **19**, 1365 (1983).

[22] J. Wiersig, J. Opt. A: Pure and Appl. Opt. **5**, 53 (2003).

[23] S. Shinohara, T. Fukushima, and T. Harayama, Phys. Rev. A **77**, 033807 (2008).